Compact Ultra-Wide-Stopband Microwave Bandpass Filter with Multiple Transmission Zeros by Integrating an L-Shaped Bandpass Filter and a Stepped Impedance Lowpass Filter

Ramkumar S., Anitha M., Student Member, IEEE, Boopathi Rani R., Senior Member, IEEE, and Muthuramya C.

***Abstract*—A compact ultra-wide-stopband microwave bandpass filter is introduced in this work using an L-shaped quarter-wavelength resonator and stepped impedance resonators. The bandpass filter (BPF-I) is designed at 2.1 GHz (f_o) using an L-shaped quarter-wavelength line. The lowpass filter is developed at 4 GHz using stepped impedance resonators. The introduced ultra-wide-stopband filter is created through integrating the BPF-I and the lowpass filter. Filter size reduction is achieved through the L-shaped quarter-wavelength line, while the ultra-wide-stopband is attained through the stepped impedance resonators. The mathematical analysis of the introduced ultra-wide-stopband bandpass filter is conducted through the extraction of ABCD and S-parameters. The lumped elements equivalent circuits are realized for the introduced filter, and their S-parameters are plotted. The introduced filter is fabricated on an FR4 substrate, and its S-parameters are measured. The comparison of mathematical analysis, EM simulated, circuit simulated, and measured results, showing good agreement. Measurements show a 140.4% fractional bandwidth (FBW), better than 20 dB return loss, higher than 28 dB rejection up to 30 GHz (14.3f_o) in the out-of-band with many transmission zeros, and 0.8 dB insertion loss. 0.23λ_g x 0.37λ_g is the overall dimension of the introduced filter.**

Link to graphical and video abstracts, and to code: https://latamt.ieeer9.org/index.php/transactions/article/view/9327

***Index Terms*— Microwave filters, multiple transmission zeros, bandpass filter, quarter-wavelength resonators, stepped impedance resonators, ultra-wide-stopband**

I. Introduction

In contemporary wireless communication systems, high-suppression and wide stopband bandpass filters (BPFs) are crucial for maintaining signal integrity and reducing interference. These filters are essential in various components, including transmitters, antennas, and power amplifiers, where they prevent unwanted signals and noise from degrading system performance. However, achieving a bandpass filter with an ultra-wide-stopband (UWSB) is challenging because the higher-order modes of microwave resonators can generate unwanted passbands, which deteriorate stopband performance.

Design approaches such as the Substrate Integrated Waveguide (SIW) technique [1], [2], [3], [4], [5], [6], Substrate Integrated Defected Ground Structure [7], Substrate Integrated Coaxial Line (SICL) [8], Integrated Passive Device technology [9], [10], [11], Multilayer PCB Technology [12], and PCB technology [13] have shown promise in achieving wide-stopband characteristics. However, these methods often increase design complexity and fabrication challenges. SIW components, for example, require precision in design and integration with other circuit elements, while Integrated Passive Device technology and Multilayer PCB Technology add to the overall design complexity.

Additionally, microstrip technologies employing various resonator configurations and techniques have been reported: open/shorted stubs [14], square stepped impedance resonators [15], quarter-wavelength stepped impedance resonators [16], modified feed structures [17], asymmetric funnel-shaped resonators [18], stepped impedance resonator with cross-coupled structure [19], two five-stage stepped impedance resonators [20], source-load coupling structure and short-stub-loaded open loop stepped-impedance resonator [21], composite right-/left-handed transmission line [22], loaded short section of parallel-coupled lines [23], middle-shorted hairpin-resonators [24], ring-shaped spoof surface plasmon polaritons (SSPPs) [25], open stub loaded dual-mode resonator [26], stepped-impedance hairpin (SIH) [27], and cascading three stepped coupled lines and two short-circuited stubs [28]. Despite these advancements, these designs achieve stopband ranges less than 5f_o (f_o- centre frequency) [14], [15], [18], [19], [22], [23], [24], [26], suffer from poor return loss [16], [19], [21], comparatively high insertion loss [27] and large size [25], [28].

In this paper, an UWSB bandpass filter utilizing L-shaped quarter-wavelength resonator and stepped impedance resonators is proposed. Initially, a bandpass filter (BPF-I) is designed using an L-shaped quarter-wavelength resonator at

The associate editor coordinating the review of this manuscript and approving it for publication was Roberto S. Murphy (*Corresponding author: Ramkumar S.*).

Ramkumar S. is with the Department of Electronics and Communication Engineering, Kumaraguru College of Technology, Coimbatore- 641049, Tamilnadu, India (e-mail: umarramk@gmail.com).

Boopathi Rani R, Anitha M, and Muthuramya C, are with the Department of Electronics and Communication Engineering, National Institute of Technology Puducherry, Karaikal-609609, Puducherry, India (e-mails: rbrani@nitpy.ac.in, anithasekaran9@gmail.com, and ramyacpct@gmail.com).

2.1 GHz. To mitigate higher-order harmonics and extend the stopband, a lowpass filter is designed at 4 GHz using stepped impedance resonators. The final proposed UWSB bandpass filter is created by integrating BPF-I and the stepped impedance lowpass filter. The created filter is fabricated on an FR4 substrate using a MITS Autolab PCB milling machine. The fabricated filter is measured with a Keysight FieldFox microwave analyzer. The measured results demonstrate a 140.4% fractional bandwidth (FBW), 20 dB return loss, wide-stopband range up to 14.3f_0 (30 GHz) with a significant rejection level of 28 dB, and 0.8 dB insertion loss. The design is compact (0.23λ_g x 0.37λ_g) and simple.

The primary contributions of this paper are as follows:

- Size reduction has been achieved by designing BPF-I using an L-shaped short-ended quarter-wavelength resonator.
- To achieve an ultra-wide-stopband and improve stopband rejection, a stepped impedance lowpass filter is designed and analyzed.
- The integration of BPF-I and the lowpass filter has been properly done to achieve a compact size, UWSB, high stopband rejection, and better impedance matching, in a single package.
- The mathematical analysis has been carried out through the extraction of ABCD and S-Parameters to validate the results analytically.
- The equivalent lumped element circuit has been extracted, designed, and the results are plotted.
- The introduced UWSB filter is fabricated, and measurements are compared with mathematical analysis, EM simulation, and circuit simulation. There is a good match in the passband responses.

The organization of this paper as follows: The BPF-I and the stepped impedance lowpass filter design and analysis are explained in Section 2. Section 3 details the introduced UWSB bandpass filter design and its corresponding analyses. Sections 4 and 5 provide the measurement results and their comparison with other works, and conclusions, respectively.

II. Design of BPF-I and LPF

A. Design of BPF-I

The quarter-wavelength resonator with one end short-circuited acts as an open circuit at the other end and vice versa. The input impedance of a short-ended quarter-wavelength line is high and inductive at the designed center frequency (f_o) [29]. Thus, it exhibits bandpass responses at f_o. Using this concept, a BPF-I is designed at 2.1 GHz using an L-shaped short ended quarter-wavelength resonator, as shown in Fig. 1. The BPF-I layout is given in Fig. 1.

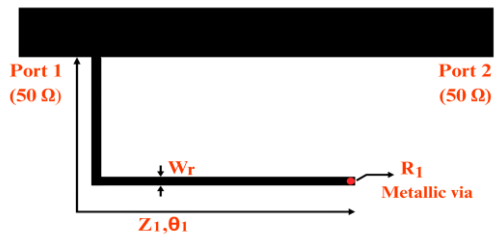

Fig. 1. Layout of BPF-I.

In Fig. 1, Port 1 and Port 2 act as the input and output terminals, respectively, and are designed for 50 Ω impedance. W_r is the quarter-wavelength resonator width, which is 0.5 mm. R_1 is the radius of the metallic via, which is 0.2 mm. The quarter-wavelength resonator characteristic impedance is Z_1 and electrical length is θ_1. Z_1 is calculated using (1).

$$Z = \frac{\eta}{2\pi\sqrt{\epsilon_{re}}}\left[8\frac{h}{w} + 0.25\frac{w}{h}\right] \quad (1)$$

where, η is the intrinsic impedance equal to 377 Ω, ϵ_{re} is the effective dielectric constant, height of the substrate, denoted as h, is 1.6 mm, while the width, represented by w, is 0.5 mm. The electrical length θ is calculated using (2).

$$\theta = \beta l \quad (2)$$

where $\beta = \frac{2\pi}{\lambda_g}$ is the phase constant, the guide wavelength is λ_g, and l is the length of the resonator. The quarter-wavelength resonator length is $\frac{\lambda_g}{4}$. The calculated value of the L-shaped quarter-wavelength resonator is 22 mm.

The BPF-I is designed and simulated using an FR4 substrate with permittivity of 4.4, thickness of 1.6 mm, and tanδ of 0.02 in HFSS. The simulated results of a BPF-I are given in Fig. 2.

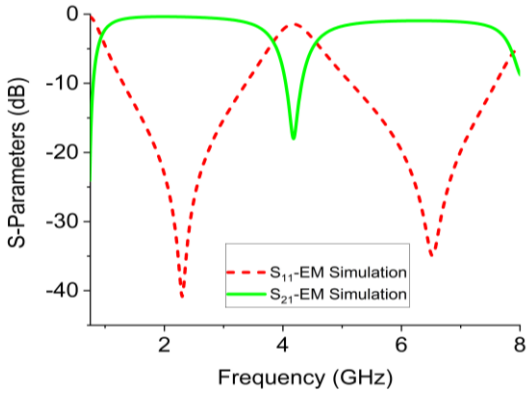

Fig. 2. Simulated S-parameters of BPF-I.

In Fig. 2, there is a higher-order harmonic at 3f_0 and poor stopband rejection. Hence, to suppress higher-order harmonics and provide wide-stopband rejection, a stepped impedance lowpass filter is included in the design, as explained in Section II. *B*.

B. Design of LPF

A sixth-order Butterworth (maximally-flat) stepped impedance lowpass filter is designed at 4 GHz using stepped impedance resonators on FR4 substrate with a permittivity of 4.4, thickness of 1.6 mm, and tanδ of 0.02. The prototype values of the sixth-order Butterworth filter are g_1=0.517, g_2=1.414, g_3=1.932, g_4=1.932, g_5=1.414, g_6=0.517 [30]. The lowpass prototype circuit is depicted in Fig. 3.

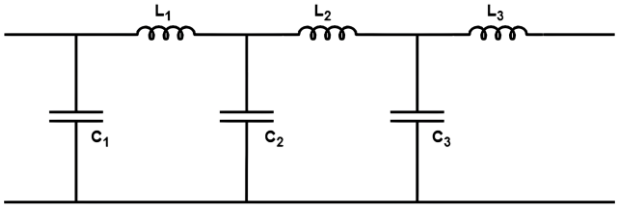

Fig. 3. Lowpass prototype circuit.

The lowpass prototype is converted into a stepped impedance lowpass filter, as shown in Fig. 4 [31].

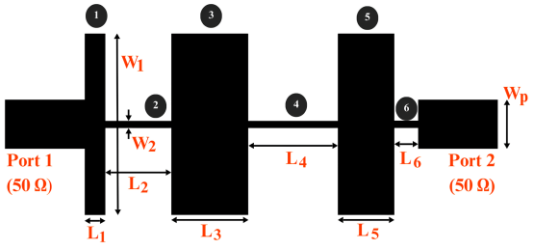

Fig. 4. Layout of the stepped impedance LPF.

In Fig. 4, resonators 1, 3, and 5 correspond to capacitor sections in the lowpass prototype circuit C_1, C_2, and C_3, and its corresponding lowpass prototype values are g_1, g_3, g_5 respectively, while resonators 2, 4, and 6 correspond to inductor sections in the lowpass prototype circuit L_1, L_2, and L_3, and its corresponding lowpass prototype values are g_2, g_4, g_6 respectively.

The length of the inductor sections is calculated using (3)

$$l = \frac{LZ_0}{\beta Z_h} \tag{3}$$

The length of the capacitor sections is calculated using (4)

$$l = \frac{CZ_l}{\beta Z_0} \tag{4}$$

The maximum line impedance, denoted as (Z_h), is 120 Ω, while the minimum line impedance, (Z_l), is 20 Ω. In (3) and (4) L and C indicates corresponding prototype values. The port impedance, Z_0, is set at 50 Ω. The lengths (in mm) of the stepped impedance lines are as follows: L_1 = 1.28, L_2 = 4.14, L_3 = 4.81, L_4 = 5.65, L_5 = 3.52, L_6 = 1.51. The widths of stepped impedance lines are W_1 = 11.3 mm and W_2 = 0.428 mm. Fig. 6 shows the plotting of the electromagnetic (EM) simulated S-parameters of the stepped impedance lowpass filter that is constructed on FR4 substrate in HFSS. The electromagnetic simulated results demonstrate a return loss of 15 dB and an insertion loss of 0.3 dB in the passband, as depicted in Fig. 6. The lowpass filter equivalent lumped element values are realized and presented in Fig. 5.

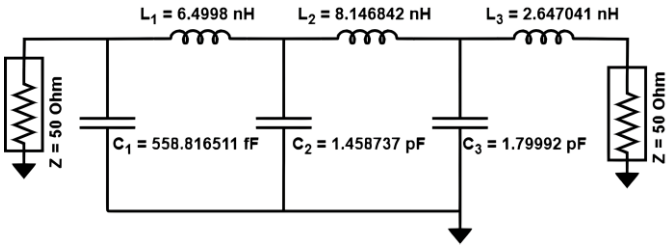

Fig. 5. Equivalent circuit of LPF.

The Advanced Design System (ADS) tool is used to construct and simulate the realized lumped element equivalent circuit, and outcomes are displayed in Fig. 6 The S-parameters of the stepped impedance lowpass filter generated through EM simulation and circuit simulation are compared in Fig. 6. There is a good agreement.

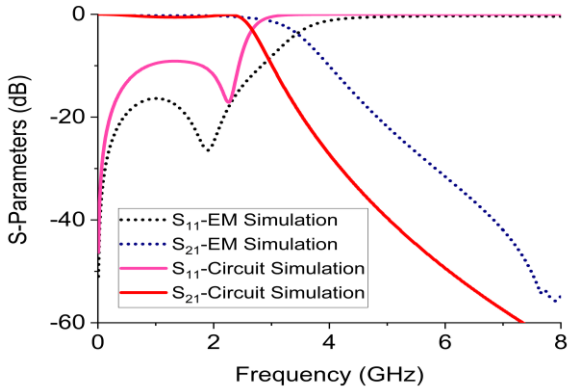

Fig. 6. S-Parameters of stepped impedance LPF with EM simulation, Circuit simulation.

III. Design of the Proposed Ultra-Wide-Stopband BPF

The proposed UWSB bandpass filter is designed by integrating the BPF-I and a stepped impedance lowpass filter. The designed BPF-I produces higher-order harmonics that can be seen in Fig. 2. To suppress higher-order harmonics BPF-I is integrated with stepped impedance lowpass filter as depicted in Fig. 7. The proposed UWSB bandpass filter layout is illustrated in Fig. 7.

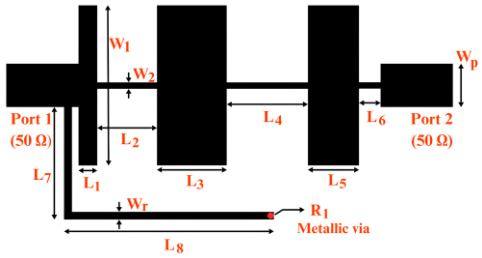

Fig. 7. Layout of the proposed ultra-wide-stopband BPF.

The proposed filter dimensions (in mm) are: W_1 = 11.3, W_2 = 0.428, W_p = 3, W_r = 0.5, L_1 = 1.28, L_2 = 4.14, L_3 = 4.81, L_4 = 5.65, L_5 = 3.52, L_6 = 1.51, L_7 = 8, and L_8 = 14. Fig. 10 shows the electromagnetic simulation results of the UWSB bandpass filter constructed on FR4 substrate.

A. Equivalent Circuit

The introduced UWSB bandpass filter equivalent lumped element circuit is realized and displayed in Fig. 8.

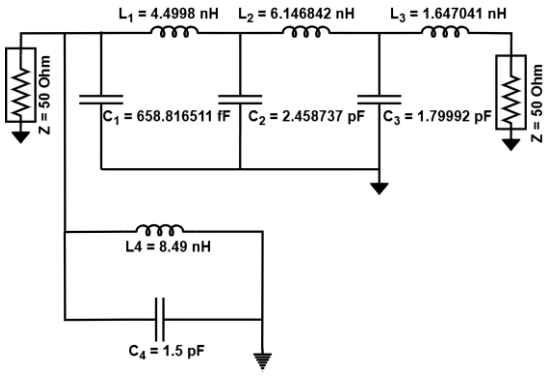

Fig. 8. Equivalent circuit of the proposed ultra-wide-stopband BPF.

The equivalent circuit is implemented and simulated using ADS software, with the resulting S-parameters illustrated in

Fig. 10.

B. Mathematical Analysis

The transmission line model for the proposed ultra-wide-stopband bandpass filter is depicted in Fig. 9.

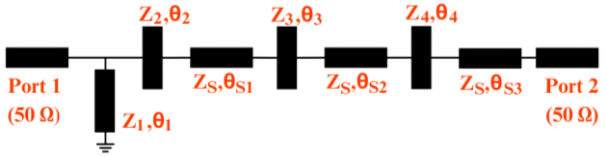

Fig. 9. Transmission line model of the proposed ultra-wide-stopband BPF.

In the transmission line model, Z_1=104.8 Ω, Z_2=77.66 Ω, Z_3= 37.24 Ω, Z_4=45.74 Ω, and Z_s=108.49 represent the impedance of the respective resonators, which are calculated using (1). The electrical lengths of the respective resonators are θ_1=96.48°, θ_2=61.26°, θ_3=64.46°, θ_{s1}=18.96°, θ_{s2}=25.88°, θ_{s3}=6.91° which are calculated at the centre frequency (f_0) using (2). The ABCD parameters of the proposed UWSB bandpass filter are arrived from Fig. 9 and given in (5).

$$\begin{bmatrix} A & B \\ C & D \end{bmatrix}_{Proposed\ BPF} = \begin{bmatrix} 1 & 0 \\ \frac{1}{jZ_1 tan\theta 1} & 1 \end{bmatrix} x \begin{bmatrix} 1 & 0 \\ \frac{j}{Z_2 cot\theta_2} & 1 \end{bmatrix} x \begin{bmatrix} cos\theta_{s1} & jZ_s sin\theta_{s1} \\ \frac{jsin\theta_{s1}}{Z_s} & cos\theta_{s1} \end{bmatrix} x \begin{bmatrix} 1 & 0 \\ \frac{j}{Z_3 cot\theta_3} & 1 \end{bmatrix} x \begin{bmatrix} cos\theta_{s2} & jZ_s sin\theta_{s2} \\ \frac{jsin\theta_{s2}}{Z_s} & cos\theta_{s2} \end{bmatrix} x \begin{bmatrix} 1 & 0 \\ \frac{j}{Z_4 cot\theta_4} & 1 \end{bmatrix} x \begin{bmatrix} cos\theta_{s3} & jZ_s sin\theta_{s3} \\ \frac{jsin\theta_{s3}}{Z_s} & cos\theta_{s3} \end{bmatrix} \quad (5)$$

Expanding (5) yields the proposed UWSB bandpass filter's ABCD Parameters. From the ABCD parameters the S-parameters of the proposed UWSB bandpass filter are derived mathematically which are provided in (6) and (7).

$$S_{11} = \frac{\begin{array}{c} -iPZ_0^2 Z_s \cos(\theta_{s3})^2 \tan(\theta_4) \\ -Z_s \sin(\theta_{s3})(Z_1 Z_2 Z_4 (YZ_0 - iXZ_s) \\ +Z_s (YZ_1 Z_2 + PZ_0 sin(\theta_{s3})) tan(\theta_4)) + \\ \cos(\theta_{s3})(PZ_0 Z_4 (-iZ_0 + Z_s) \sin(\theta_{s3}) \\ +Z_1 Z_2 Z_s (YZ_4 + XZ_0 Z_4 - YZ_0 Z_s tan(\theta_4))) \end{array}}{\begin{array}{c} -iPZ_0^2 Z_s \cos(\theta_{s3})^2 \tan(\theta_4) \\ +Z_s \sin(\theta_{s3})(Z_1 Z_2 Z_4 (-YZ_0 + iXZ_s) \\ +(-Z_s YZ_1 Z_2 + PZ_0 Z_s sin(\theta_{s3})) tan(\theta_4)) \\ +\cos(\theta_{s3})(iPZ_0 Z_4 (Z_0 + iZ_s) \sin(\theta_{s3}) \\ +Z_1 Z_2 Z_s (YZ_4 + XZ_0 Z_4 - YZ_0 Z_s tan(\theta_4))) \end{array}} \quad (6)$$

$$S_{21} = \frac{2Z_0 Z_1 Z_2 Z_3 Z_4 Z_s}{\begin{array}{c} iPZ_0^2 Z_s \cos(\theta_{s3})^2 \tan(\theta_4) \\ +Z_s \sin(\theta_{s3})(Z_1 Z_2 Z_4 (-YZ_0 + iXZ_s) \\ +(-Z_s YZ_1 Z_2 + PZ_0 Z_s sin(\theta_{s3})) tan(\theta_4)) \\ +\cos(\theta_{s3})(iPZ_0 Z_4 (Z_0 + iZ_s) \sin(\theta_{s3}) \\ +Z_1 Z_2 Z_s (YZ_4 + XZ_0 Z_4 - YZ_0 Z_s tan(\theta_4))) \end{array}} \quad (7)$$

where, $X = cos(\theta_{s1})cos(\theta_{s2})sin(\theta_{s1})(Z_3 sin(\theta_{s2}) + Z_s cos(\theta_{s2}) tan(\theta_3))$,

$$Y = Z_3 cos(\theta_{s2}) sin(\theta_{s1}) + sin(\theta_{s2})(Z_3 cos(\theta_{s1}) - Z_s sin(\theta_{s1}) tan(\theta_3)),$$

$$\begin{array}{l} P = Z_3 sin(\theta_{s2})\, Z_s sin(\theta_{s1})(Z_2 cot(\theta_1) - Z_1 \tan(\theta_2))) + \\ \cos(\theta_{s2})(Z_3(Z_1(Z_2 \sin(\theta_{s1})(-Z_2 Z_s \cot(\theta_1) + \\ Z_1 Z_s tan\theta_2))) + Z_s(Z_1 Z_2 \cos(\theta_{s2}) + \\ Z_s \sin(\theta_{s1})(Z_2 \cot(\theta_1) - Z_1 \tan(\theta_2)))\tan(\theta_3)) + \\ (\sin(\theta_{s1})(Z_3 Z_s \cos(\theta_{s2}) Z_2 \cot(\theta_1) - Z_1 \tan(\theta_2)) - \\ \sin(\theta_{s2})(Z_1 Z_2 Z_3 + Z_s^2 \cot(\theta_1)\tan(\theta_3) - \\ Z_1 Z_s^2 \tan(\theta_2)\tan(\theta_3))) + \quad cos(\theta_{s1})(Z_1 Z_2 Z_3 cos(\theta_{s2}) + \\ Z_s sin(\theta_{s2})(Z_2 Z_3 cot(\theta_1) - Z_1(Z_3 tan(\theta_2) + Z_2 tan(\theta_3))))). \end{array}$$

The S-parameters of the proposed UWSB bandpass filter are mathematically analyzed and plotted using (6) and (7) as a function of frequency, as depicted in Fig. 10.

IV. Measurement Results and Discussion

The FR4 substrate with permittivity of 4.4, tanδ of 0.02, and thickness of 1.6 mm, and is used to fabricate the introduced UWSB bandpass filter. The measured results are evaluated against the results from EM simulations, circuit simulations, and mathematical analyses, as shown in Fig. 10.

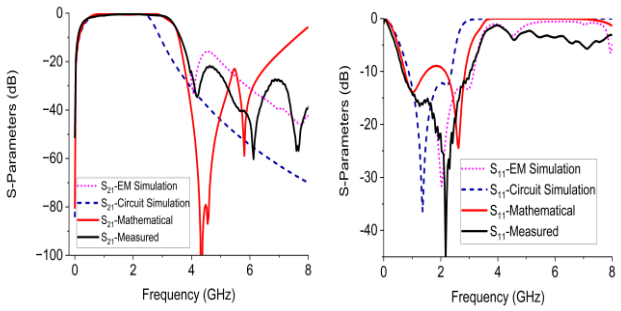

(a) (b)

Fig. 10. S-Parameters of the ultra-wide-stopband BPF with EM simulation, Circuit simulation, Mathematical and Measured: (a) S_{21} (b) S_{11}.

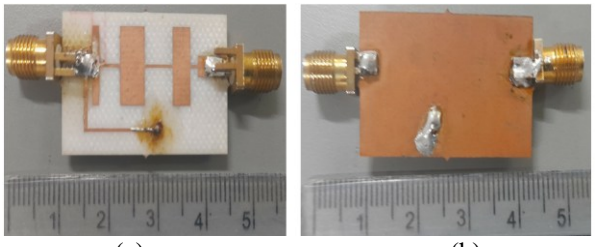

(a) (b)

Fig. 11. The photograph of the fabricated filter: (a) Top view (b) Bottom view.

Fig. 11 shows the photograph of fabricated prototype. The fabricated prototype is validated through measured results using Keysight microwave analyzer. The measurement setup is shown in Fig. 12.

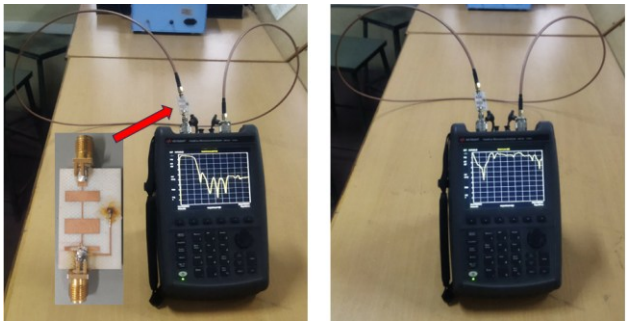

(a) (b)

Fig. 12. The photograph of the measurement setup: (a) S_{21} (b) S_{11}.

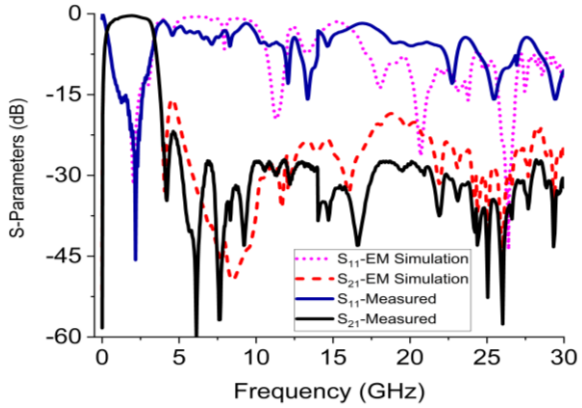

Fig.13. S-Parameters of the ultra-wide-stopband BPF with EM simulation and measured results up to 14.3f_0.

The compared results show good agreement in the passband, as seen in Fig. 10. The simulated results and measured results are compared up to 30 GHz and presented in Fig. 13. The measured results show a 140.4% FBW, better than a 20 dB return loss, 0.8 dB insertion loss, in the passbands, and better than a 28 dB rejection in the stopband up to 14.3f_0. Multiple transmission zeros appear at 4.2 GHz, 6 GHz, 7.6 GHz, 8.3 GHz, 9.2 GHz, 10.5 GHz, 11.2 GHz, 12.18 GHz, 14 GHz, 14.7 GHz, 16.6 GHz, 21.9 GHz, 23 GHz, 24.3 GHz, 25 GHz, 26 GHz, 27.7 GHz, and 29.3 GHz, enhancing the upper stopband rejection. Fig. 14 shows that the group delay of the introduced filter is consistently flat and shows less than 0.8 ns.

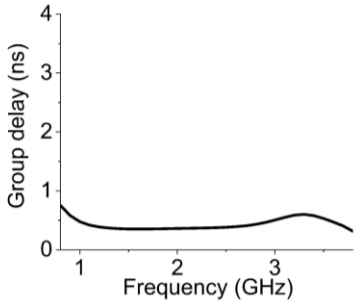

Fig. 14. The group delay of the proposed filter.

The comparison of the proposed work with other work is shown in TABLE I. The comparison reveals that the introduced UWSB bandpass filter achieves an ultra-wide stopband extending up to 14.3f_0, surpassing the performance of all other filters outlined in TABLE I. The proposed filter demonstrates a high rejection level of 28 dB, which is higher than all other works in TABLE I except [15], [23], [24]. It also shows a very good return loss of 20 dB and multiple transmission zeros compared to all other proposed works in TABLE I. Additionally, the insertion loss is low compared to most of the already proposed works and features a compact size.

TABLE-I
THE PERFORMANCE OF THE PROPOSED WORK COMPARED WITH OTHER WORKS.

Ref. No.	Centre frequency f_0 (GHz)	Stopband width / Rejection level (dB)	Insertion loss(dB)	Fractional bandwidth (FBW) (%)	Return loss (dB)	TZs	Size (λ_g^2)
[15]	1.26	3.5f_0 / 50	1.8	5.6	15.6	NA	0.42 × 0.3
[16]	2.02	13.86f_0 / 22.2	1.15	17.5	10	2	0.22 × 0.18
[17]	1.415	8.2f_0 / 20	1.42	9.3	20	9	0.16 × 0.211
[18]	5.68	4.3f_0 / 20	1.62	97.57	20	6	0.3157
[19]	2.45	4.1f_0 / 20	1.2	10	11	3	0.161×0.128
[20]	6.95	14.4f_0 / 17.5	0.42	97	19	3	0.128×0.378
[21]	2.4	8.3f_0 / 21.2	NA	4	11	3	NA
[22]	6.85	4.38f_0 / 18	0.9	110.9	13	3	0.22 × 0.20
[23]	2.45	2.8f_0 / 32	0.3	35	12	3	NA
[24]	5.4	3f_0 / 30	1.2	11.4	20	3	0.5 × 0.35
[25]	3.5	8.6f_0 / 25	1	85.71	15	NA	1.13 × 0.23
This work	2.1	14.3f_0 / 28	0.8	140.4	20	18	0.23 × 0.37

TZ: Transmission zero, NA; Not available in the Paper

V. CONCLUSION

In the proposed work, an ultra-wide-stopband bandpass filter is designed, simulated, and fabricated. The proposed UWSB bandpass filter is designed by integrating the BPF-I and the stepped impedance lowpass filter. The equivalent lumped element circuit of the introduced filter is realized and designed in ADS software, and the S-parameters are plotted. The mathematical analysis of the filter is performed by its transmission line model through the ABCD and S-parameters derivation, with results plotted. The results of mathematical analysis, circuit simulation, and electromagnetic simulation are compared with the measured results, showing good agreement. The proposed UWSB bandpass filter has an overall dimension of $0.23\lambda_g$ x $0.37\lambda_g$. The performance of the proposed filter is compared with other filters, demonstrating an ultra-wide-stopband with high rejection levels, lower insertion loss, multiple transmission zeros, better return loss, and a compact size with a simple design. The proposed UWSB bandpass filter is well-suited for the L band and S band applications.

REFERENCES

[1] P. Kim and Y. Jeong, "Compact and wide stopband substrate integrated waveguide bandpass filter using mixed quarter-and one-eighth modes cavities," *IEEE Microw Wirel Compon Lett*, vol. 30, no. 1, pp. 16-19, Dec. 2019. doi: 10.1109/LMWC.2019.2954603.

[2] H. Y. Xie, B. Wu, L. Xia, J. Z. Chen, and T. Su, "Miniaturized half-mode fan-shaped SIW filter with extensible order and wide stopband," *IEEE Microw Wirel Compon Lett*, vol. 30, no. 8, pp. 749-752, Jun. 2020. doi: 10.1109/LMWC.2020.3001092.

[3] Y. Zheng, H. Tian, Y. Dong, and Y. Wu, "Miniaturized, Wide Stopband Filter Based on Shielded Capacitively Loaded SIW Resonators," *Chin J Electron*, vol. 33, no. 2, pp. 456-462, Mar. 2024. doi: 10.23919/cje.2023.00.057.

[4] P. Chu, J. Feng, P. Zhu, L. Guo, F. Zhu, K. L. Zheng, L. Liu, and K. Wu, "Substrate Integrated Waveguide Filter with Wide Stopband Up to (2k + 3) f0," *IEEE Trans Microw Theory Tech*, vol. 71, no. 12, pp. 5358–5366, Dec. 2023, doi: 10.1109/TMTT.2023.3313868.

[5] P. Chu, J. Feng, P. Zhu, L. Guo, L. Zhang, L. Liu, G. Luo, K. Wu, and S. Pan, "Wide Stopband Substrate Integrated Waveguide Filter Using Bisection and Trisection Coupling in Multilayer," *Chin J Electron*, vol. 33, no. 2, pp. 436-442, Mar. 2024. doi: 10.23919/cje.2023.00.027.

[6] C. X. Zhou, P. P. Guo, K. Zhou, and W. Wu, "Design of a compact UWB filter with high selectivity and superwide stopband," *IEEE Microw Wirel Compon Lett*, vol. 27, no. 7, pp. 636-638, Jul. 2017. doi: 10.1109/LMWC.2017.2711509

[7] J. Zhou, Y. Rao, D. Yang, H. J. Qian, and X. Luo, "Compact wideband BPF with wide stopband using substrate integrated defected ground structure," *IEEE Microw Wirel Compon Lett*, vol. 31, no. 4, pp. 353-356, Feb. 2021. doi: 10.1109/LMWC.2021.3053756.

[8] P. Chu, L. Guo, L. Zhang, and K. Wu, "Wide stopband bandpass filter implemented by stepped impedance resonator and multiple in-resonator open stubs," *IEEE Access*, vol. 7, pp. 140631-140636, Sep. 2019. doi: 10.1109/ACCESS.2019.2943605.

[9] V. B. Narayane and G. Kumar, "A selective wideband bandpass filter with wide stopband using mixed lumped-distributed circuits," *IEEE Trans Circuits Syst II Express Briefs*, vol. 69, no. 9, pp. 3764-3768, May 2022. doi: 10.1109/TCSII.2022.3173472.

[10] Y. Jiang, L. Feng, H. Zhu, W. Feng, H. Chen, Y. Shi, W. Che, and Q. Xue, "Bandpass filter with ultra-wide upper stopband on GaAs IPD technology," *IEEE Trans Circuits Syst II Express Briefs*, vol. 69, no. 2, pp. 389-393, Jul. 2021. doi: 10.1109/TCSII.2021.3096936.

[11] B. G. Liu, Y. J. Zhou, and C. H. Cheng, "Miniaturized ultra-wideband bandpass filter with ultra-wide stopband using π-type unit with inductive loading on integrated passive device," *IEEE Trans Circuits Syst II Express Briefs*, vol. 68, no. 11, pp. 3406-3410, May 2021. doi: 10.1109/TCSII.2021.3078154.

[12] Y. Rao, H. J. Qian, J. Zhou, Y. Dong, and X. Luo, "Miniaturized 28-GHz packaged bandpass filter with high selectivity and wide stopband using multilayer PCB technology," *IEEE Microw Wirel Compon Lett*, vol. 32, no. 6, pp. 664-667, Apr. 2022. doi: 10.1109/LMWC.2022.3163613.

[13] B. A. Belyaev, A. M. Serzhantov, Y. F. Bal'va, R. G. Galeev, and A. A. Leksikov, "Design for a self-packaged all-PCB wideband filter with good stopband performance," *IEEE Trans Compon Packag Manuf Technol*, vol. 12, no. 7, pp. 1186-1195, Jul. 2022.

[14] X. Gao, W. Feng, and W. Che, "Compact ultra-wideband bandpass filter with improved upper stopband using open/shorted stubs," *IEEE Microw Wirel Compon Lett*, vol. 27, no. 2, pp. 123-125, Feb. 2017.

[15] R. Y. Yang, C. M. Hsiung, C. Y. Hung, and C. C. Lin, "A high performance bandpass filter with a wide and deep stopband by using square stepped impedance resonators," *J Electromagn Waves Appl*, vol. 24, no. 11-12, pp. 1673-1683, Jan. 2010. doi: 10.1163/156939310792149722.

[16] M. Hayati, H. Asadbeigi, and A. Sheikhi, "Design of microstrip quasi-elliptic bandpass filter with upper wide stopband using quarter-wavelength stepped-impedance resonators," *Electromagn.*, vol. 33, no. 7, pp. 507-516, Oct. 2013. doi: 10.1080/02726343.2013.824310.

[17] D. Li, J. A. Wang, Z. Chen, Y. Zhang, M. C. Tang, and L. Yang, "Compact microstrip bandpass filter with sharp roll-off and broad stopband using modified 0° feed structure *AEU - Int. J Electron Commun*, vol. 109, pp. 17-22, Sep. 2019. doi: 10.1016/j.aeue.2019.06.030.

[18] Iqubal and P. Abdulla, "Bandpass filter based on asymmetric funnel shaped resonators with ultrawide upper stopband characteristics," *AEU - Int. J Electron Commun*, vol. 116, p. 153062, Mar. 2020. doi: 10.1016/j.aeue.2020.153062.

[19] J. Sheen, Y. H. Cheng, and W. Liu, "Design of a microwave bandpass filter with compact size and wide stopband," *Microw Opt Technol Lett*, vol. 55, no. 8, pp. 1860-1863, Aug. 2013. doi: 10.1002/mop.27720.

[20] Sheikhi, A. Alipour, and A. Mir, "Design and fabrication of an ultra-wide stopband compact bandpass filter," *IEEE Trans Circuits Syst II Express Briefs*, vol. 67, no. 2, pp. 265-269, Mar. 2019. doi: 10.1109/TCSII.2019.2907177.

[21] H. W. Deng, Y. J. Zhao, W. Chen, B. Liu, and Y. Y. Liu, "Wide upper-stopband microstrip bandpass filter with dual-mode open loop stepped-impedance resonator and source-load coupling structure," *Microw Opt Technol Lett*, vol. 54, no. 7, pp. 1618-1621, Jul. 2012. doi: 10.1002/mop.26881.

[22] J. Zeng, X. Li, and Z. Qi, "UWB bandpass filter with compact size and wide upper stopband," *Microw Opt Technol Lett*, vol. 62, no. 4, pp. 1521-1525, Apr. 2020. doi: 10.1002/mop.32200.

[23] J. Marimuthu, A. M. Abbosh, and B. Henin, "Bandpass filter with wide stopband using loaded short-section of parallel-coupled lines," *Microw Opt Technol Lett*, vol. 57, no. 12, pp. 2824-2829, Dec. 2015. doi: 10.1002/mop.29441.

[24] Ramkumar S and R. Boopathi Rani, "Compact high-selective wide-stopband coupled bandpass filter using middle-shorted hairpin-resonators," *AEU - Int. J Electron Commun*, vol. 162, p. 154580, Apr. 2023. doi: 10.1016/j.aeue.2023.154580.

[25] B. Ren, W. Chen, X. Guan, and S. Wan, "Compact bandpass filter with ultra-wide stopband based on spoof surface plasmon polaritons for sub-6G application," *AEU - Int. J Electron Commun*, vol. 176, p. 155152, Mar. 2024. doi: 10.1016/j.aeue.2024.155152.
[26] H. W. Deng, Y. J. Zhao, X. S. Zhang, L. Zhang, and S. P. Gao, "Compact wide upper-stopband BPF using open stub loaded dual-mode resonator," *Microw Opt Technol Lett*, vol. 52, no. 10, pp. 2185-2188, Oct. 2010. doi: 10.1002/mop.25453.
[27] M. H. Ho and W. C. Lin, "Design of stepped-impedance hairpins band-pass filter with wide stopband performance *Microw Opt Technol Lett*, vol. 52, no. 6, pp. 1405-1408, Jun. 2010. doi: 10.1002/mop.25179.
[28] C. W. Tang and C. H. Teng, "A wide stopband microstrip bandpassfilter with stepped coupled lines," *Microw Opt Technol Lett*, vol. 56, no. 10, pp. 2283-2286, Oct. 2014. doi: 10.1002/mop.28569.
[29] Ramkumar S and R. Boopathi Rani, "Compact reconfigurable bandpass filter using quarter wavelength stubs for ultra-wideband applications," *AEU - Int. J Electron Commun*, vol. 151, p. 154219, Jul. 2022. doi: 10.1016/j.aeue.2022.154219.
[30] L. Young and G. Matthaei, *Microwave filters, impedance matching networks and coupling structures*, Artech House, 1980, pp.97-98.
[31] D. Pozar, *Microwave Engineering*, 4th ed. John Wiley & Sons, 2017, p.424.

Ramkumar S received his B.E. (2012) and M.E. (2014) in Electronics and Communication Engineering from Anna University, Chennai, and completed his Ph.D. in 2023 from NIT Puducherry. He has worked as a Research Scientist at SAMEER, Ministry of Electronics and IT, Government of India. His research focuses on wireless communication, microwave filters, reconfigurable filters, filter-integrated antennas, RF energy harvesting, and UWB filters. Additionally, he holds an M.A. in Yoga for Human Excellence from Tamil University, Thanjavur**.**

Anitha M (Student Member, IEEE) received her B.E. in Electronics and Communication Engineering (2016) and M.E. in Applied Electronics (2018) from Anna University, Chennai. She is currently pursuing her Ph.D. at NIT Puducherry, focusing on satellite communication, air pollution studies, and the prediction of aerosol parameters using machine learning and deep learning.

Boopathi Rani R (Senior Member, IEEE) holds a B.E. in Electronics and Communication Engineering from Bharathidasan University and an M.E. in Communication Systems from Anna University, where she secured University First Rank. She earned her Ph.D. in antennas from NIT Puducherry and is currently an Assistant Professor at NIT Puducherry, with over a decade of academic experience and 60+ research publications. She has received several awards, including the Best Teacher Award (2007) and ISTE's Best Women Engineering College Teacher (2010). She is a Fellow of IETE, ATMS, and a member of ISTE and SEMCE(I).

Muthuramya C received her B.E. in Electronics and Communication Engineering (2009) and M.E. (2011) from Anna University, and earned her Ph.D. in antennas from NIT Puducherry (2022). She served as an Assistant Professor at SCAD College of Engineering and Technology, Tirunelveli, from 2012 to 2019, with 11 national and international research publications. Her research interests include wireless communication, miniaturized antennas, fractal antennas, UWB antennas, and super-wideband antennas.